

Aberration correction for direct laser written waveguides in a transverse geometry

L. Huang,¹ P. S. Salter,¹ F. Payne,¹ and M. J. Booth^{1,2,*}

¹*Department of Engineering Science, University of Oxford, Parks Road, Oxford, OX1 3PJ, UK*

²*Centre for Neural Circuits and Behaviour, University of Oxford, Mansfield Road, Oxford, OX1 3SR, UK*

[*martin.booth@eng.ox.ac.uk](mailto:martin.booth@eng.ox.ac.uk)

Abstract: The depth dependent spherical aberration is investigated for ultrafast laser written waveguides fabricated in a transverse writing geometry using the slit beam shaping technique in the low pulse repetition rate regime. The axial elongation of the focus caused by the aberration leads to a distortion of the refractive index change, and waveguides designed as single mode become multimode. We theoretically estimate a depth range over which the aberration effects can be compensated simply by adjusting the incident laser power. If deeper fabrication is required, it is demonstrated experimentally that the aberration can be successfully removed using adaptive optics to fabricate single mode optical waveguides over a depth range > 1 mm.

Published by The Optical Society under the terms of the [Creative Commons Attribution 4.0 License](#). Further distribution of this work must maintain attribution to the author(s) and the published article's title, journal citation, and DOI.

OCIS codes: (010.1080) Active or adaptive optics; (140.3390) Laser materials processing; (230.7370) Waveguides; (090.1000) Aberration compensation; (070.6120) Spatial light modulators.

References and links

1. K. M. Davis, K. Miura, N. Sugimoto, and K. Hirao, "Writing waveguides in glass with a femtosecond laser," *Opt. Lett.* **21**, 1729 – 1731 (1996).
2. G. D. Valle, R. Osellame, and P. Laporta, "Micromachining of photonic devices by femtosecond laser pulses," *J. Opt. A: Pure Appl. Opt.* **11**, 013001 (2009).
3. N. Huot, R. Stoian, A. Mermillod-Blondin, C. Mauclair, and E. Audouard, "Analysis of the effects of spherical aberration on ultrafast laser-induced refractive index variation in glass," *Opt. Express* **15**, 12395–12408 (2007).
4. S. Gross and M. J. Withford, "Ultrafast-laser-inscribed 3d integrated photonics: challenges and emerging applications," *Nanophotonics* **4**, 2192 (2015).
5. S. Eaton, H. Zhang, M. Ng, J. Li, W. Chen, S. Ho, and P. Herman, "Transition from thermal diffusion to heat accumulation in high repetition rate femtosecond laser writing of buried optical waveguides," *Opt. Express* **16**, 9443–9458 (2008).
6. Y. Cheng, K. Sugioka, K. Midorikawa, M. Masuda, K. Toyoda, M. Kawachi, and K. Shihoyama, "Control of the cross-sectional shape of a hollow microchannel embedded in photostructurable glass by use of a femtosecond laser," *Opt. Lett.* **28**, 55–57 (2003).
7. G. Cerullo, R. Osellame, S. Taccheo, M. Marangoni, D. Polli, R. Ramponi, P. Laporta, and S. DeSilvestri, "Femtosecond micromachining of symmetric waveguides at 1.5 μm by astigmatic beam focusing," *Opt. Lett.* **27**, 1938–1940 (2002).
8. M. Ams, G. D. Marshall, and M. J. Withford, "Study of the influence of femtosecond laser polarisation on direct writing of waveguides," *Opt. Express* **14**, 13158–13163 (2006).
9. F. He, H. Xu, Y. Cheng, J. Ni, H. Xiong, Z. Xu, K. Sugioka, and K. Midorikawa, "Fabrication of microfluidic channels with a circular cross section using spatiotemporally focused femtosecond laser pulses," *Opt. Lett.* **35**, 1106 – 1108 (2010).

10. V. Diez-Blanco, J. Siegel, A. Ferrer, A. R. de la Cruz, and J. Solis, "Deep subsurface waveguides with circular cross section produced by femtosecond laser writing," *Appl. Phys. Lett.* **91**, 051104 (2007).
11. C. Mauchair, A. Mermillod-Blondin, N. Huot, E. Audouard, and R. Stoian, "Ultrafast laser writing of homogeneous longitudinal waveguides in glasses using dynamic wavefront correction," *Opt. Express* **16**, 5481–5492 (2008).
12. A. Marcinkevicius, V. Mizeikis, S. Juodkakis, S. Matsuo, and H. Misawa, "Effect of refractive index-mismatch on laser microfabrication in silica glass," *Appl. Phys. A* **76**, 257–260 (2003).
13. C. Hnatovsky, R. S. Taylor, E. Simova, V. R. Bhardwaj, D. M. Rayner, and P. B. Corkum, "High-resolution study of photoinduced modification in fused silica produced by a tightly focused femtosecond laser beam in the presence of aberrations," *Jnl. Appl. Phys.* **98**, 013517 (2005).
14. Q. Sun, H. Jiang, Y. Liu, Y. Zhou, H. Yang, and Q. Gong, "Effect of spherical aberration on the propagation of a tightly focused femtosecond laser pulse inside fused silica," *J. Opt. A: Pure Appl. Opt.* **7**, 655–659 (2005).
15. A. Jesacher, G. D. Marshall, T. Wilson, and M. J. Booth, "Adaptive optics for direct laser writing with plasma emission aberration sensing," *Opt. Express* **18**, 656–661 (2010).
16. M. J. Booth, M. A. A. Neil, and T. Wilson, "Aberration correction for confocal imaging in refractive-index-mismatched media," *Journal of Microscopy* **192**, 90–98 (1998).
17. B. Sun, P. S. Salter, and M. J. Booth, "Effects of aberrations in spatiotemporal focusing of ultrashort laser pulses," *J. Opt. Soc. Am. A* **31**, 765–772 (2014).
18. R. R. Thomson, T. A. Birks, S. G. Leon-Saval, A. K. Kar, and J. Bland-Hawthorn, "Ultrafast laser inscription of an integrated photonic lantern," *Opt. Express* **19**, 5698–5705 (2011).
19. R. Heilmann, R. Keil, M. Gräfe, S. Nolte, and A. Szameit, "Ultraprecise phase manipulation in integrated photonic quantum circuits with generalized directional couplers," *Appl. Phys. Lett.* **105**, 061111 (2014).
20. J. Grenier, L. Fernandes, J. Aitchison, P. Marques, and P. Herman, "Femtosecond laser fabrication of phase-shifted bragg grating waveguides in fused silica," *Opt. Lett.* **37**, 2289–2291 (2012).
21. J. B. Spring, P. S. Salter, B. J. Metcalf, P. C. Humphreys, M. Moore, N. Thomas-Peter, M. Barbieri, X.-M. Jin, N. K. Langford, W. S. Kolthammer, M. J. Booth, and I. A. Walmsley, "On-chip low loss heralded source of pure single photons," *Opt. Express* **21**, 13522–13532 (2013).
22. Y. Duan, P. Dekker, M. Ams, G. Palmer, and M. Withford, "Time dependent study of femtosecond laser written waveguide lasers in yb-doped silicate and phosphate glass," *Opt. Mat. Express* **5**, 416–422 (2015).
23. A. Crespi, R. Osellame, R. Ramponi, D. J. Brod, E. F. Galvo, N. Spagnolo, C. Vitelli, E. Maiorino, P. Mataloni, and F. Sciarrino, "Integrated multimode interferometers with arbitrary designs for photonic boson sampling," *Nat. Photonics* **7**, 545549 (2013).
24. P. S. Salter, A. Jesacher, J. B. Spring, B. J. Metcalf, N. Thomas-Peter, R. D. Simmonds, N. K. Langford, I. A. Walmsley, and M. J. Booth, "Adaptive slit beam shaping for direct laser written waveguides," *Opt. Lett.* **37**, 470–472 (2012).
25. Y. Liao, J. Qi, P. Wang, W. Chu, Z. Wang, L. Qiao, and Y. Cheng, "Transverse writing of three-dimensional tubular optical waveguides in glass with slit-shaped femtosecond laser beams," *arXiv p. 1602.01570* (2016).
26. A. Jesacher, P. S. Salter, and M. J. Booth, "Refractive index profiling of direct laser written waveguides: tomographic phase imaging," *Opt. Mat. Express* **3**, 1223–1232 (2013).
27. R. Arimoto and J. M. Murray, "A common aberration with water immersion objective lenses," *J. Microscopy* **216**, 49–51 (2004).
28. B. Sun, P. S. Salter, and M. J. Booth, "Effects of sample dispersion on ultrafast laser focusing," *J. Opt. Soc. Am. B* **32**, 1272–1280 (2015).
29. T. Fernandez, J. Siegel, J. Hoyo, B. Sotillo, P. Fernandez, and J. Solis, "Controlling plasma distributions as driving forces for ion migration during fs laser writing," *J. Phys. D: Appl. Phys.* **48**, 155101 (2015).
30. N. Jovanovic, P. Tuthill, B. Norris, S. Gross, P. Stewart, N. Charles, S. Lacour, M. Ams, J. Lawrence, A. Lehmann, C. Niel, J. Robertson, G. Marshall, M. Ireland, A. Fuerbach, and M. Withford, "Starlight demonstration of the dragonfly instrument: an integrated photonic pupil-remapping interferometer for high-contrast imaging," *MN-RAS* **427**, 806–815 (2012).
31. D. MacLachlan, R. Harris, D. Choudhury, R. Simmonds, P. Salter, M. J. Booth, J. R. Allington-Smith, and R. R. Thomson, "Development of integrated mode reformatting components for diffraction-limited spectroscopy," *Opt. Lett.* **41**, 76–79 (2016).
32. A. Szameit, J. Burghoff, T. Pertsch, S. Nolte, A. Tunnermann, and F. Lederer, "Two-dimensional soliton in cubic fs laser written waveguide arrays in fused silica," *Opt. Express* **14**, 6055–6062 (2006).
33. D. Guzman-Silva, C. Mejia-Cortes, M. Bandres, M. Rechtsman, S. Weimann, S. Nolte, M. Segev, A. Szameit, and R. Vicencio, "Experimental observation of bulk and edge transport in photonic lieb lattices," *New Journal of Physics* **16**, 063061 (2014).
34. S. Mukherjee, A. Spracklen, D. Choudhury, N. Goldman, P. Ohberg, E. Andersson, and R. R. Thomson, "Observation of a localized flat-band state in a photonic lieb lattice," *Phys. Rev. Lett.* **114**, 245504 (2015).

1. Introduction

Ultrafast direct laser writing (DLW) is a powerful technique that can be used to fabricate three-dimensional (3D) waveguides and other optical elements in transparent materials [1,2]. Ideally, a tightly-focused circular beam is required for the DLW fabrication. If the shape of the focus is impaired, the quality of the written waveguides is affected [3]. Maintaining waveguide circularity, symmetry and mode-field profiles are challenges that can limit the coupling loss and 3D capability of the ultrafast laser-writing technique [4].

When writing waveguides with a low pulse repetition rate laser ($\lesssim 100$ kHz), outside of the cumulative heating regime [5], the cross-section of the resultant structure tends to be closely matched to the shape of the focal intensity distribution. In a transverse writing geometry (moving the sample perpendicular to the beam-propagation direction), the focal spot has a naturally elliptical profile. The waveguides can thus be highly elliptical in cross section. Through careful beam preparation, such as beam shaping [6–8] or spatio-temporal focusing [9], a disc-shaped focus may be generated to give symmetric waveguides. However, such symmetry is still destroyed by depth dependent aberrations, which can greatly limit the capability of 3D laser fabrication at greater depths [10, 11].

A spherical aberration (SA) is induced when focusing light through a refractive-index interface [12–14]. Typically, when a laser beam is focused from air into a sample with a refractive index n , refraction at the interface leads to an optical path length (OPL) difference between beams incident at different angles. The aberration becomes more severe for larger n and higher numerical aperture (NA). Thus, a low NA objective ($NA \approx 0.2$) may be used to minimise the depth dependent spherical aberration, but the associated highly asymmetric focal cross-section leads to large mode area waveguides [10]. For DLW waveguides with efficient coupling to single mode fibre, a higher NA ~ 0.5 is required and the depth range is limited to a fraction of a millimetre from the surface.

In this paper, we initially explore theoretically the effects of spherical aberration related to waveguide fabrication over different depth ranges. Subsequently we demonstrate experimentally correction of the depth-dependent spherical aberration via adaptive optics to fabricate single-mode waveguides at different focusing depths in fused silica. A spatial light modulator (SLM) is implemented into the DLW system to provide dynamic control in phase modulation for both beam-shaping and aberration correction. The plasma emission sensing method [15] is used to ensure the optimum focus is achieved at each depth. We show that the proposed technique greatly improves the focal quality at greater depths and facilitated the fabrication of more accurate and controllable 3D laser-written waveguides.

2. Aberrations for waveguides

For an appropriately aligned optical system, the only aberration to be considered when writing waveguides inside isotropic materials is the depth dependent spherical aberration SA. By considering the change in optical path length for rays refracted at the surface of the material, the phase in the pupil of the objective lens associated with the SA can be written as [16]:

$$\phi_{SA}(\rho) = \frac{-2\pi d_{nom}}{\lambda} \left(\sqrt{n^2 - (NA\rho)^2} - \sqrt{1 - (NA\rho)^2} \right) \quad (1)$$

where λ is the wavelength of the light, ρ is the normalised pupil radius, n is the refractive index of the sample and d_{nom} is the nominal depth within the sample [Fig. 1(a)]. It is assumed that the objective lens is operating in air ($n = 1$). This SA phase can be separated into a component which distorts the focal intensity and another which refocuses the optical system. It is instructive to estimate the depth ranges over which it is expected that this aberration will not adversely

affect the waveguide writing process. Therefore, the three dimensional intensity distribution at the focus is calculated for a range of depths within a glass substrate for which $n = 1.45$. The focal intensity is simulated using a scalar approximation based upon a Fourier optics calculation [17]. Beam shaping to achieve a symmetric focal disc is implemented in the simulation by placing a slit of width w in the pupil, where w is dependent on the objective NA and focal length. At each depth within the glass, two parameters are extracted: the peak intensity I_p and the full width half maximum Δ_z of the distribution in the z (beam propagation) direction. The results are plotted in Fig. 1 for three different numerical apertures relevant for waveguide writing.

From inspection of Eq. (1), it can be seen that the aberration is heavily dependent on the numerical aperture of the objective. An objective with numerical aperture of 0.4 is routinely used for waveguide writing [18, 19] and is largely robust to the depth dependent spherical aberration. From Fig. 1(b), the focal intensity only drops by a tenth over a 400 μm depth range. This of course can be compensated by increasing the input laser power to the system, of greater consequence is the change in the axial extent of the focus Δ_z which affects the waveguide morphology. Over the same depth range, Δ_z only increases by $\sim 10\%$, indicating that it should be possible to successfully write waveguides without the aberration proving too detrimental. At greater depths, it may be expected that the waveguide morphology changes substantially.

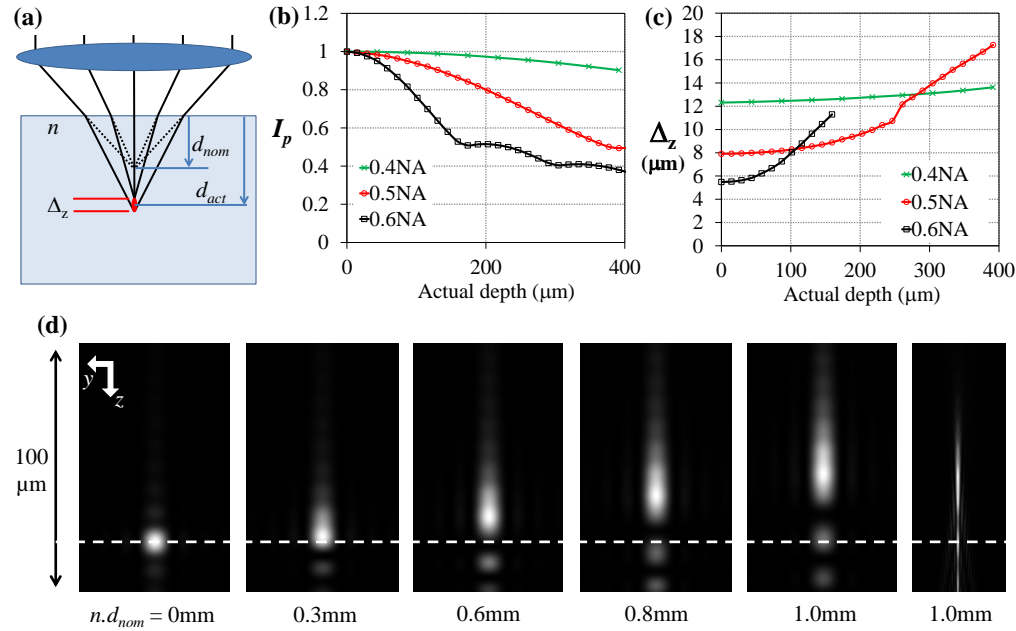


Fig. 1. (a) Schematic of the focussing geometry. (b) Simulated estimate of the drop in the peak focal intensity I_p as a function of the depth beneath the surface of the glass. (c) Increase in the axial extent of the focal intensity Δ_z as a function of depth. (d) For a 0.5 NA lens, the simulated focal intensity cross sections at various depths. The intensity scale in each image is individually normalised. The laser is incident along the z direction, and in the simulation there is a slit oriented along the y direction masking the pupil intensity. The white dashed line indicates the stated z position for each image, which is equal to nd_{nom} . At a depth of 1 mm, the simulation is also shown for the case where there is no slit beam shaping and full pupil illumination is used.

For some applications [5, 20–23], it is necessary to generate waveguides with smaller cross-section and hence to write with a lens of higher NA. Figures 1(b),(c) reveal that the effect of the aberration starts to become much more relevant at NA = 0.5 and 0.6. At 0.6 NA, Δ_z changes by 10 % over a distance of less than 50 μm , presenting significant challenges for three dimensional waveguide circuits. Note that the curve for 0.6 NA lens in Fig. 1(c) is terminated at a depth of 150 μm , since at greater depths the focus is so distorted that defining an axial FWHM becomes meaningless. The 0.5 NA lens offers approximately a range of 140 μm over which the axial focal extent remains relatively undistorted, accompanied by a small drop in peak intensity that should be compensated to maintain waveguide uniformity. It is interesting to note that should one require to fabricate over a depth range greater than 250 μm , it would be best to use the 0.4NA objective lens regardless of desired feature size. It is also worth noting that often objective lenses designed for use in the life sciences are internally corrected to remove the aberration arising from a 170 μm coverslip. In such a case these quoted depth ranges should be viewed as the distance above and below the 170 μm depth that can be successfully accessed, thus increasing the overall ‘aberration-free’ range.

In Fig. 1(d), the simulated effect of the aberration for a 0.5 NA lens is demonstrated at depths greater than 300 μm . The images show a cross-section through the focal disc created by slit-beam shaping. Two effects are apparent as one moves to greater depths. Firstly, the focus becomes distorted such that the cross-section is no longer symmetric and substantially larger in the axial direction. The expected end result would be that waveguides supporting a single mode at shallow depths become multimode deeper within the glass. Secondly, the exact axial position of the waveguide becomes difficult to predict, with the actual depth of the peak intensity being less than nd_{nom} . The accurate fabrication of 3D waveguide circuits thus becomes more complicated.

3. Waveguide fabrication

Having theoretically explored the range over which aberrations are relevant for waveguide fabrication, we now experimentally demonstrate the effects of aberrations and how they may be corrected to facilitate the fabrication of 3D waveguide circuits over a millimetre depth range. Figure 2(a) shows the schematic diagram of our laser fabrication system. The laser was a regeneratively amplified Ti-sapphire laser (Solstice-100F, Newport/Spectra Physics), operating at a repetition rate of 1 kHz with 100 fs pulses centred at a wavelength of 790 nm. The pulse energy was controlled by a rotatable half-wave plate ($\lambda/2$) and a subsequent Glan-Laser polariser. The beam was then expanded and directed to a spatial light modulator (SLM Hamamatsu Photonics X10468-02). The SLM was imaged to the pupil plane of the microscope objective (20 \times , Zeiss Plan Neofluar with 0.5 NA), which had an internal correction for a 170 μm coverglass. The specimen was on a computer-controlled three axis translation stage (Aerotech ABL10100 and ANT95-3-V). The focal region was imaged during fabrication through a dichroic mirror onto a CCD.

Prior to any aberration correction, an initial phase pattern shown in Fig. 2(b) was applied onto the SLM screen. It comprised three main components: the blazed grating, slit and background phase pattern. The background phase pattern was used to correct the initial flatness of the SLM and the system aberration. The blazed grating was used to efficiently diffract light to the first order, reducing interference with other unmodulated light from the SLM. A pinhole of diameter 500 μm was placed in the Fourier plane of the SLM as a spatial filter, only passing light which was in the first diffracted order of the grating [24, 25]. The pinhole should be large enough (greater than $\approx 200 \mu\text{m}$) to avoid any additional spatial filtering of the shaped focus. The slit was used to obtain a symmetric waveguide cross-section by reducing the size of the grating, and hence the effective NA of the system, in one dimension. Experimental measurements of

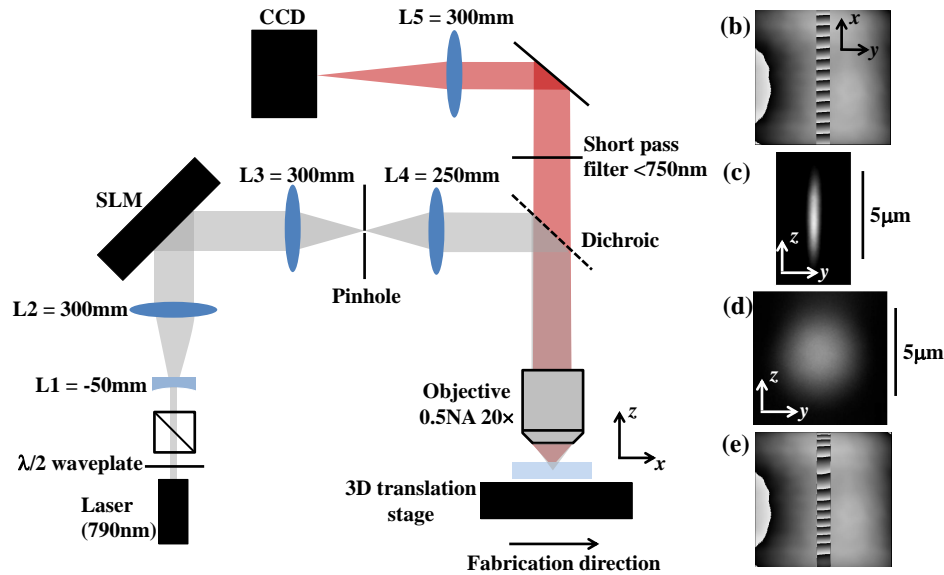


Fig. 2. (a) Schematic diagram of the ultrafast laser fabrication system. Lens (L1-L4) focal lengths are shown in mm. Some intermediate optics have been omitted for clarity. (b) A phase pattern applied on an SLM screen for beam-shaping. (c) Original focus dimensions without an SLM. (d) Experimental measurement of the focus with circular cross-section after beam-shaping using the SLM. (e) Modified SLM phase pattern showing a distorted grating to give an aberration corrected circular focus at a depth of 1.0 mm.

the resulting laser writing focus, Fig.2(d), showed a circular transverse profile compared to the original focus without beam-shaping [Fig. 2(c)].

Laser pulses were focused 0.2 mm–1.2 mm below the surface of a 1.35 mm thick fused silica specimen ($10 \times 1.35 \times 10$ mm). All waveguides were fabricated at a speed of $25 \mu\text{m/s}$ along the x-direction (perpendicular to the laser optic-axis) at a length of 10 mm. At each depth the pulse energy was carefully adjusted to ensure the maximum index contrast, ascertained via in-situ phase microscopy [26], without cracking the glass. Slit beam-shaping [24] and aberration correction based on the plasma emission method [15] were both applied on the SLM to achieve a symmetric focal-disc for fabrication.

For characterisation, a laser beam at a wavelength of 630 nm from a single mode fibre was butt-coupled in air to the written waveguides and the end facet of the output near-field mode was captured by using a long-working distance (LWD) microscope objective lens attached to a charge-coupled device (CCD) camera. The end surfaces of the fused silica were carefully polished after waveguide fabrication to ensure minimum loss.

4. Plasma emission aberration sensing

Initially the aberration was minimised at each depth through applying a phase pattern to the SLM based on Eq. (1). The plasma emission aberration sensing method was then employed to adaptively update the applied phase. During laser fabrication, a plasma is generated at the laser focus by multi-photon absorption and avalanche effects. The super-continuum emitted by the focal plasma was imaged during fabrication and the intensity used as a metric for optimisation of the focal spot quality using a sensorless adaptive optics protocol [15]. A well aberration-corrected focal spot corresponds to the maximum plasma emission.

Following a similar procedure to that described in [15], orthogonal modes from a Zernike basis were selected to apply differing magnitudes of aberration to incident laser. For each mode, the magnitude corresponding to maximum plasma emission was found. The phase pattern of the SLM was thus updated at each depth to fine tune the aberration correction. Small adjustments to the predicted phase [Eq. (1)] were required from the spherical Zernike modes corresponding to potential deviation in pupil size and numerical aperture of the objective lens from its stated values. Also small amounts of astigmatism and coma were applied; these can be attributed to the correction of effects arising from a small tilt in the workpiece relative to the optic axis [27]. We note that the slit beam shaping reduces the number of Zernike modes relevant for aberration correction since there is minimal phase variation across the width of the slit [17].

4.1. Waveguides at different depths

Waveguides were fabricated using the proposed method with and without adaptive aberration correction at five different depths: 0.17, 0.4, 0.7, 0.9 and 1.0 mm corresponding to nominal refocusing depths of 0.115, 0.275, 0.48, 0.62 and 0.7 mm respectively. The phase pattern before aberration correction comprised the blazed grating, the slit and the background phase pattern, as described before. There was an additional additional aberration correction phase applied on the SLM for each depth based on the results of the plasma emission sensing. An example of the applied phase is shown in Fig. 2(e), where it can be seen that the grating used to generate the slit beam shaping is distorted. It is important that the aberration correction is only applied to the grating region of the SLM, so that the filtering of the zero order by the pinhole is unaffected.

Figure 3 shows images of the aberration-uncorrected waveguides fabricated at various depths of 0.17, 0.4, 0.7, 0.9 and 1.0 mm in a fused silica specimen viewed under a transmission microscope. All the waveguides were written at the same speed of 25 $\mu\text{m/s}$ with different pulse energies for different depths. The pulse energy should be carefully chosen by rotating the angle of the half-wave plate at the laser output to provide sufficient modification without severe damage. In agreement with the theoretical predictions of Section 2, we found that the written waveguide cross-section was not greatly modified over a depth range of 0.17 ± 0.15 mm provided the power was appropriately modified. Without aberration correction at greater depths, focal spot became highly aberrated, resulting in non-circular and non-homogenous waveguides with larger cross-section. The simulated focal cross-sections from Fig. 1(d) are in good qualitative agreement with the fabricated cross-sections, bearing in mind the objective is internally corrected for a microscope coverslip such that a depth of 0.17 mm should be considered ‘aberration-free’ in experiment.

Conversely, when an aberration correction is applied as shown in Fig. 4, observable circular and homogenous waveguides could be created in the focal region at different depths. The cross-sectional profile and dimensions of the waveguides are maintained through various depths.

Note that a higher pulse energy was required for refractive-index modification at larger depths. The required pulse energy increased from 4.9 μJ (at a depth of 0.17 mm) to 9.9 μJ (at a depth of 1.0 mm), when no aberration correction was applied. The increased pulse energy requirement is mainly caused by the depth-dependent aberration, which highly extends the dimensions of the writing focus. We note that we were not able to fabricate symmetric waveguides at great depth by carefully tuning the incident laser power to overcome the effects of the aberration. From inspection of Fig. 1 (d), this should in principle be possible, but it is very difficult to get the level of control necessary for consistent fabrication. When aberration correction was applied, there was much less increase in pulse energy (3.9 μJ to 5.8 μJ) over the same 1.0 mm depth range. The residual rise in pulse energy was related to the limited diffraction efficiency of the SLM and difficulty in perfectly compensating the aberration. We have previously shown theoretically that dispersion should not be important when propagating a 100 fs pulse through

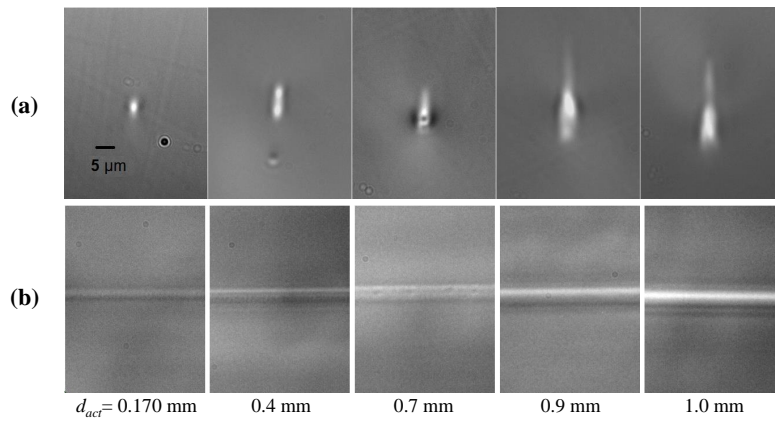


Fig. 3. Transmission microscope images of waveguides fabricated at different depths without aberration correction, viewed from (a) the end facet and (b) above. Images are contrast adjusted to increase visualization.

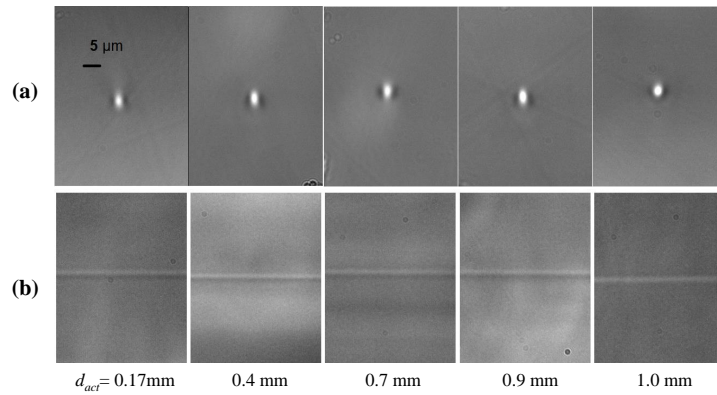


Fig. 4. Transmission microscope images of waveguides fabricated at different depths with aberration correction, viewed from (a) the end facet and (b) above. Images are contrast adjusted to increase visualization.

this depth of fused silica [28] but, non-linear effects can not be discounted.

The aberration correction can also help with precise placement of the waveguide position inside the sample. Figure 5 shows that, at the depth of 1.0 mm, the uncorrected waveguides are closer to the surface from the original set position, whereas the corrected ones are circular and precisely located at a depth of $d_{act} = nd_{nom} = 1.45 \cdot 0.7 = 1.015$ mm. Furthermore, it was observed that there was much greater repeatability in the depth positioning of the waveguides when the aberration was compensated. For the deepest guides, there was a variation of $6 \mu\text{m}$ in depth for five successive guides fabricated in identical conditions without aberration correction. This is presumably related to nonlinear propagation resulting from the higher required pulse energy. When aberration correction was applied, the depth variation dropped to below $1 \mu\text{m}$.

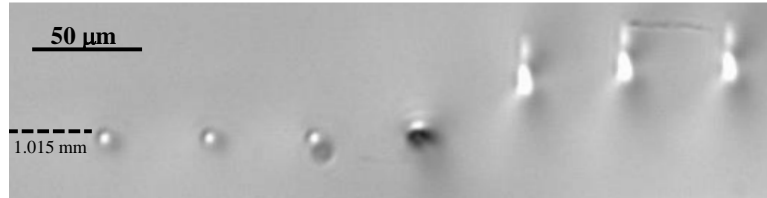


Fig. 5. Transmission microscope image of waveguides fabricated at a depth 1.0 mm. The left three waveguides were aberration corrected, whereas the right three were aberration uncorrected. The central marker splitting the two sets is a region of laser induced damage.

When coupling the light into the uncorrected waveguides at different depths [Fig. 6(a)], multi-mode guiding was observed, especially for those at greater depths. However, waveguides fabricated with aberration correction resulted in much better quality with more confined circular cross-sections, and were single-mode [Fig. 6(b)]. The corrected waveguides fabricated at the depth of 1.0 mm had similar quality and profile as the ones at a lower depth of 0.17 mm. This indicates that the focal spot was well aberration-corrected during fabrication.

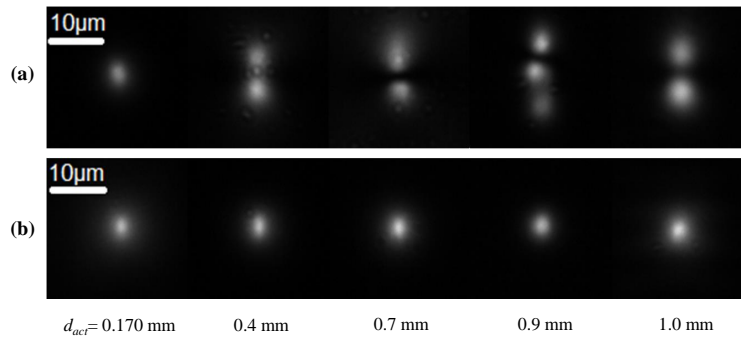


Fig. 6. The near-field intensity distribution for a wavelength of 630 nm at the output face of the fabricated waveguide chip for guides written without (a) and with (b) aberration correction.

Using quantitative phase microscopy via the TIE method [26], a refractive index increase of approximately $3\text{--}5 \times 10^{-3}$ was estimated for the aberration corrected waveguides. The magnitude of the refractive index change was strongly dependent upon the incident laser power, but with aberration correction could be maintained at different depths. Phase microscopy via the TIE only gives a one dimensional measure of the optical path length accumulated for light,

and consequently it is difficult from a single measurement to ascertain the peak index change for the asymmetric waveguides written at great depth without aberration correction. However, the peak index change could be seen as approximately consistent whether aberration correction was applied or not- i.e. it has a far greater dependency on the material and laser parameters than any focal distortion. This was in agreement with measurements of the propagation loss of the waveguides, which was estimated as approximately 1.2 dB/cm at the test wavelength of 630 nm. Within the measurement uncertainty the overall propagation loss was independent of the fabrication depth and the aberration correction. The primary benefit of the aberration correction was to maintain uniform waveguide cross-section and hence single mode operation at all depths within the glass.

5. Conclusion

In conclusion, we have explored theoretically the range over which depth-dependent aberrations are important for waveguide writing in glass at three commonly used numerical apertures. Waveguides with a uniform cross-section may be expected over a depth range of 400, 140 and 50 μm for objective lenses with NAs of 0.4, 0.5 and 0.6 respectively, provided that the incident laser fabrication power is appropriately adjusted. This work considers waveguide writing in a low pulse repetition rate (PRR) regime with slit beam shaping, and we expect the results to be highly analogous for waveguides with cross-sections tailored by other methods, such as astigmatic focal shaping [7], spatio-temporal focusing [9] or using the multiscan technique [18]. It is more difficult, however, to predict the effect of the aberration on waveguide writing at higher PRR, corresponding to a cumulative heating regime where the waveguide cross-section is not so closely matched to the focal intensity [5]. Indeed, it has recently been shown that induced spherical aberration can aid waveguide writing in such systems by driving ion migration [29].

Experimentally we have demonstrated waveguides by laser writing at depths up to 1.2 mm in fused silica at a 0.5 NA. At depths greater than 0.35 mm, the quality of the laser-written waveguides was highly affected by the depth-dependent aberration, and could be greatly improved using adaptive aberration correction. Waveguides deep below the surface are highly asymmetric with irregular cross-sections. These waveguides require higher power for sufficient refractive-index modification and become multi-mode. By applying adaptive optics in our DLW system, the corrected waveguides had circular symmetric profiles and the single-mode were well-confined during transmission. Similar waveguide profiles and performances over a large depth range were maintained, while more accurate and predictable position control could be achieved. The experimental results showed that the aberration correction could greatly facilitate the fabrication of high-quality waveguides over large depth ranges. These results are expected to be important for DLW waveguide circuits that comprise waveguides at multiple depths, for example in devices for photonic reformatting [18, 30, 31] or waveguide lattices [32–34].

Acknowledgments

The authors gratefully acknowledge the Engineering and Physical Sciences Research Council (grant numbers EP/E055818/1 and EP/K034480/1) and the Leverhulme Trust for financial support.